Full C-Band 3060-km DMD-Unmanaged 3-Mode Transmission With 40.2-Tb/s Capacity Using Cyclic Mode Permutation

Kohki Shibahara, *Member, IEEE*, Takayuki Mizuno, *Member, IEEE*, Hiroto Kawakami, *Member, IEEE*, Takayuki Kobayashi, *Member, IEEE*, Masanori Nakamura, Kota Shikama, *Member, IEEE*, Kazuhide Nakajima, *Member, IEEE*, and Yutaka Miyamoto, *Member, IEEE*

(Top-Scored Paper)

***Abstract*—We have achieved the longest three mode-multiplexed full C-band transmission yet attained over 3060 km. In wideband mode-multiplexed transmission over weakly-coupled fewmode fibers (FMFs), the width of signal impulse responses is dependent on wavelength, and also exhibits a linear growth with increased transmission distance because of the presence of differential mode delay (DMD). Those properties are technically challenging issues for future deployable space division multiplexing (SDM) transport systems since they make a system design complicated, especially for terrestrial FMF transmission links. In this article, we describe how we applied a cyclic mode permutation (CMP) technique to achieve wideband long-haul FMF transmission where spatial channels are cyclically interchanged in each span to suppress DMD-induced pulse broadening. The CMP technique enabled DMD-unmanaged long-haul transmission across 4.4-THz optical bandwidth over two-mode FMF whose DMD varied in the range from 33.7–44.3 ps/km, resulting in 3060-km FMF transmission with a net capacity of 40.2 Tb/s.**

***Index Terms*—Cyclic mode permutation (CMP), differential mode delay (DMD), space division multiplexing (SDM).**

I. Introduction

OVERWHELMING traffic growth has driven significant research efforts for the development of SDM technology in the last decade [1]. The capability of accommodating extremely high capacity has been shown in SDM transmission experiments using multicore fibers (MCFs) [2], [3] and multicore fewmode fibers (FMFs) [4]. Exploiting spatial modes in FMFs as parallelized information-carrying optical waveguides is beneficial for enhancing spatial channels up to 45 [5] for FMFs and more than 100 for MC-FMFs [4], [6]. Recently, high-capacity and long-haul FMF transmission demonstrations have been reported including 159-Tb/s transmission over 1045-km 3-mode fiber using the C+L bands [7] and 138-Tb/s transmission over 590-km 6-mode fiber using the C band [8].

Mode division multiplexed (MDM) signal performance is significantly dominated by certain physical phenomena that arise in FMF transmission lines. Especially, in weakly-coupled MDM transmission where signals are transmitted with a low mixing ratio between non-degenerate modes, signal impulse responses are broadened in an almost linear fashion with increased transmission distance, yielding a pulse spread as large as several tens of ns. This effect stems from differential mode delay (DMD), and has a negative impact especially on the computational complexity of multiple-input multiple-output digital signal processing (MIMO-DSP) that is responsible for undoing modal mixing and DMD effects in the digital domain. One approach for mitigating the impact of DMD is building a DMD-compensated transmission line by managing DMD profiles of FMFs. Known as the DMD-management technique, this approach enhanced achievable transmission reach to over 1000 km [7], [9]. Since a DMD slope property along a wavelength is sensitive to fiber parameters including refractive index profiles of a fiber [10], a challenging issue for DMD-managed FMF transmission is the stringent design constraint in terrestrial FMF transmission links that inhibits controlling span-by-span wavelength-dependent DMD characteristics.

The introduction of transmission regime with strong intermodal mixing is an approach for achieving DMD-unmanaged long-haul MDM transmission. This can be substantially achieved in SDM transmission over coupled-core MCFs [11], or over FMFs where mode mixing techniques (e.g., long-period grating techniques [12], [13] are applied. We previously proposed a mode-permutation strategy that significantly mitigates modal dispersion effects even in a weakly-coupled FMF transmission line and hence achieved 6300-km 3-mode

Manuscript received June 13, 2019; revised September 12, 2019, September 30, 2019, and October 15, 2019; accepted October 16, 2019. Date of publication October 30, 2019; date of current version January 23, 2020. *(Corresponding author: Kohki Shibahara.)*

K. Shibahara, T. Mizuno, H. Kawakami, T. Kobayashi, M. Nakamura, and Y. Miyamoto are with NTT Network Innovation Laboratories, NTT Corporation, Yokosuka 239-0847, Japan (e-mail: kouki.shibahara.nv@hco.ntt.co.jp; takayuki.mizuno.zp@hco.ntt.co.jp; hiroto.kawakami.xy@hco.ntt.co.jp; takayuki.kobayashi.wt@hco.ntt.co.jp; masanori.nakamura.cu@hco.ntt.co.jp; yutaka.miyamoto.fb@hco.ntt.co.jp).

K. Shikama is with NTT Device Technology Laboratories, NTT Corporation, Atsugi 243-0198, Japan (e-mail: kouta.shikama.bc@hco.ntt.co.jp).

K. Nakajima is with NTT Access Network Service Systems Laboratories, NTT Corporation, Tsukuba 305-0805, Japan (e-mail: kazuhide.nakajima.gr@hco.ntt.co.jp).

Color versions of one or more of the figures in this article are available online at http://ieeexplore.ieee.org.

Digital Object Identifier 10.1109/JLT.2019.2950430

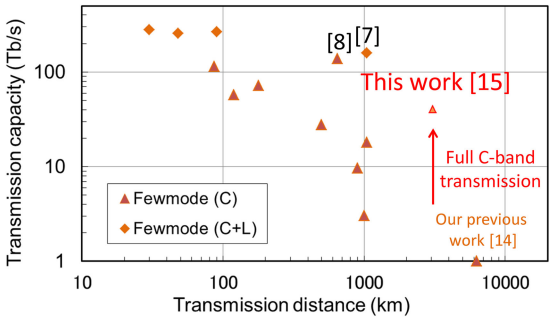

Fig. 1. Transmission distance vs. capacity in FMF transmission experiments using the C or C+L bands.

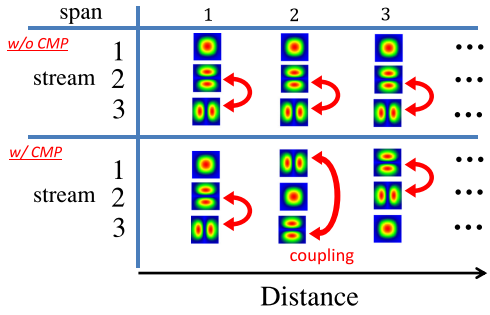

Fig. 2. Schematics of MDM transmission without (top) and with (bottom) the CMP scheme over 2LP-mode FMF transmission line.

transmission [14]. This paper is an extension of our previous one [15] with more detailed discussion on experimental results including properties of signal impulse responses, mode dependent loss, and optical signal-to-noise ratio (OSNR). In [15] we demonstrate that we were able to achieve the longest full C-band 3-mode transmission yet achieved without using a DMD-management approach (Fig. 1). Transmission with CMP suppressed DMD-induced pulse spreading in all wavelength/spatial channels where DMD values ranged from 33.7 to 44.3 ps/km over the entire C-band, achieving 3060-km FMF transmission with a net capacity of 40.2 Tb/s.

II. DMD-Unmanaged Wideband FMF Transmission Using Cyclic Mode Permutation Technique

With the aim of achieving DMD-unmanaged long-haul FMF transmission, we previously proposed a novel transmission scheme that we termed cyclic mode permutation (CMP). In a transmission strategy with the CMP scheme, span-by-span spatial channel interchange is carried out in a cyclic manner via a pair of mode-selective multiplexer/demultiplexer (MUX/DEMUX). By introducing transmission with CMP strategy, we could expect two significant effects: First expectation is that information symbols delivered on each spatial channel would periodically experience all optical paths being characterized by each spatial mode. Secondly, signal pulses launched on specific spatial mode is coupled with degenerate modes during propagation over FMFs. The combined effects described above would bring quasi strongly-coupled transmission even in weakly-coupled FMF transmission lines. Fig. 2 explains these effects when a CMP technique is used over 2LP-mode FMFs. The initial experimental evaluation we performed [14] revealed that the CMP scheme allowed us to perform the first-ever *DMD-unmanaged* long-haul MDM transmission where the required equalizer tap number in MIMO-DSP was greatly reduced by 50% in 2500-km MC-FMF transmission using optical bandwidth of 1 nm.

In the work we report in this paper, we further applied the CMP scheme to a full C-band application to demonstrate long-haul wideband FMF transmission without managing DMD. Recently-achieved MDM transmission using FMFs or MC-FMFs are listed in Table I with their experimental parameters. One can readily calculate the equalizer window width by the

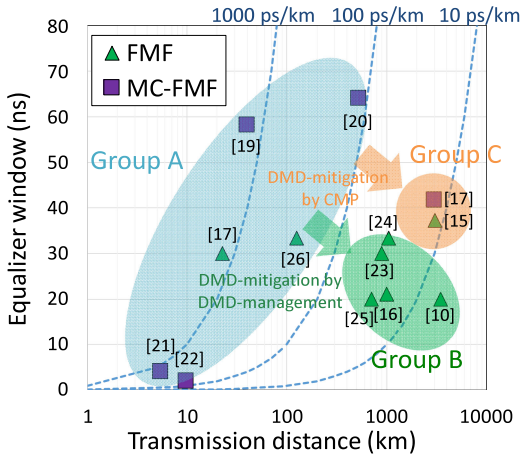

Fig. 3. Equalizer window required for MIMO-DSP in recently-reported MDM transmission experiments.

product of the inverse of symbol rates and equalizer tap numbers. Note that equalizer tap numbers in the table are resized to symbol-spaced ones. Fig. 3 maps these transmission experiments in terms of equalizer window and transmission distance. Broken lines in the figure show the equalizer window per unit length (10, 100, and 1000 ps/km). Then we categorize them into two groups A, and B. Group A contains MDM transmission experiments where equalizer window exceeding 100 ps/km was required. The main reason of enhanced equalizer window width is an employment of an SDM fiber with higher core counts and/or higher-order modes. The rest of MDM transmission experiments was categorized as group B. The MDM signal transmission with narrower equalizer window was performed in these experiments, because they mostly constructed a transmission fiber to minimize total DMD (i.e., DMD-management approach) except for [16]. Therefore DMD-management approach is considered to be useful to suppress DMD accumulation. Next we added our experimental results of the DMD-unmanaged MDM transmission employing CMP scheme [15], [17] on the figure as the third group C. We found that CMP scheme also provides a significant DMD-impact mitigation effect in MDM transmission not only over a FMF [15] but also over MC-FMF [17], from which we consider that CMP scheme is a promising enabler to realize long-haul SDM transport systems using MDM technology.

TABLE I
MIMO-DSP PARAMETERS IN RECENT MDM TRANSMISSION EXPERIMENTS

Ref.	SDM Fiber	Number of spatial modes	Transmission distance (km)	Symbol rate (GBd)	Number of equalizer taps	Equalizer window (ns, calculated)
[16]	FMF	3	1000	19	400	21.1
[18]	FMF	3	900	30	900	30
[19]	FMF	3	1050	30	1000	33.3
[9]	FMF	3	3500	30	600	20
[15]	FMF	3	3060	12	448	37.3
[20]	FMF	6	708	20	400	20
[21]	FMF	10	125	30	1000	33.3
[22]	FMF	15	22.8	30	900	30
[23]	MMF	36	2	15	1000	66.7
[5]	MMF	45	26.5	15	300	20
[24]	MC-FMF	3	40.4	0.525	30	58.1
[25]	MC-FMF	3	527	1	64	64
[26]	MC-FMF	3	5.5	25	100	4
[27]	MC-FMF	6	9.8	10	20	2
[17]	MC-FMF	3	3004	6	250	41.7

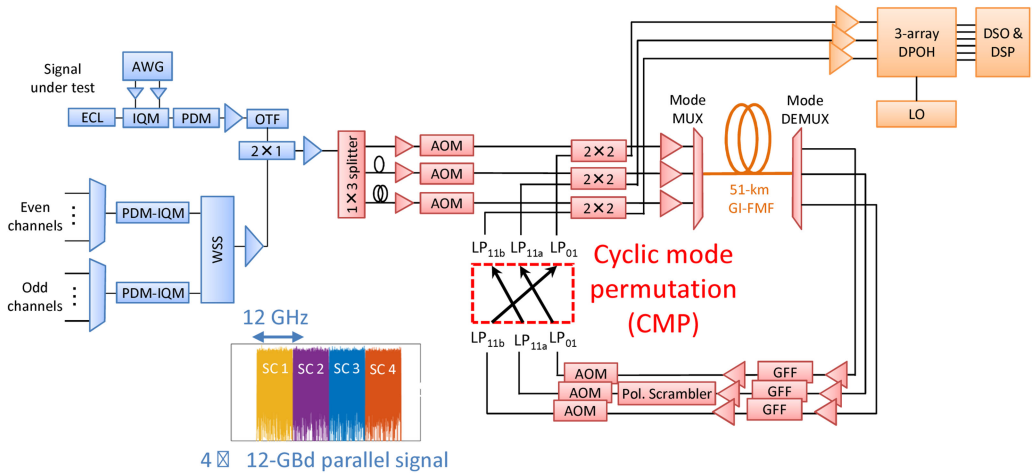

Fig. 4. Experimental setup. Inset shows a signal spectrum of fourfold subcarriers.

III. EXPERIMENTAL SETUP

We conducted a long-haul FMF transmission experiment by using the experimental setup shown in Fig. 4. At the transmitter, a test channel was generated by an 84-GSa/s arbitrary waveform generator (AWG), an IQ-modulator, and a polarization division multiplexing (PDM) emulator with 87.6-ns delay. Additional even/odd channels ranging from 1529.553 to 1564.679 nm were independently generated. The channels were combined by a wavelength selective switch (WSS) and a 2×1 optical coupler to yield 50-GHz-spaced 89 wavelength devision multiplexed (WDM) PDM-QPSK channels. The WDM channels were then split into three and delayed by 202 ns for the LP_{11a} input and 404 ns for the LP_{11b} input relative to the LP_{01} input. The binary pattern was coded with an low density parity check (LDPC) code defined in the digital video broadcasting satellite second generation (DVB-S2) standard. The code rate was set to 9/10, 5/6, 4/5, 3/4, and 2/3 depending on wavelength channels. We also assumed a 7%-overhead (OH) continuously-interleaved Bose Chaudhuri and Hocquenghem (CI-BCH) code [28] as an outer forward error correction (FEC) code to remove residual bit errors after LDPC decoding. The transmission frame was a 263,680 symbol-length QPSK pattern per spatial channel containing 0.42%-OH for the training sequence. We employed a parallel signal transmission in which four subcarriers were digitally combined into a single 50-GHz signal bandwidth. Each subcarrier was driven at 12 Gbaud with 0.15-GHz subcarrier spacing. Note that the generated parallel signal was equivalent to a 48 ($=12 \times 4$)-Gbaud carrier signal with gross bitrate of 192 Gb/s, which is the highest baud-rate signal ever employed in reported FMF transmission experiments.

Then a threefold recirculating loop system was constructed to examine the transmission performance of MDM signals. The system comprised a MUX/DEMUX mode pair, a transmission fiber, EDFAs, a loop-synchronous polarization scrambler, gain-flattening filters (GFFs), and AOMs. The transmission fiber was a 51 km-long graded-index (GI) FMF having a DMD of >33.7 ps/km, and an effective area (A_{eff}) of 111 μm^2 for the LP_{01} mode. The GFF profile for each recirculating loop was independently optimized. The loop length of each recirculating loop system was well arranged to have a length

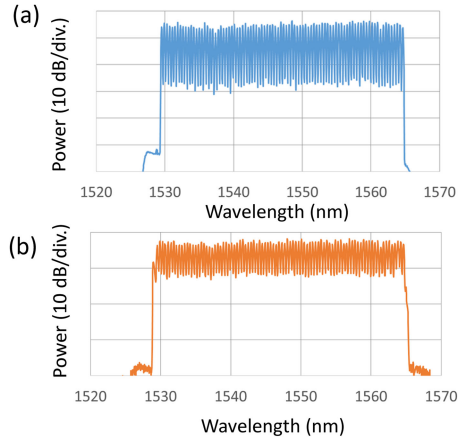

Fig. 5. Optical spectrums at the LP_{11a} output (a) before and (b) after 3060-km FMF transmission.

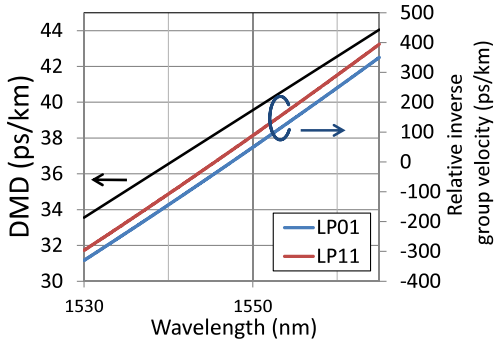

Fig. 6. Measured DMD and relative inverse group velocity for LP_{01} and LP_{11} modes across the entire C band.

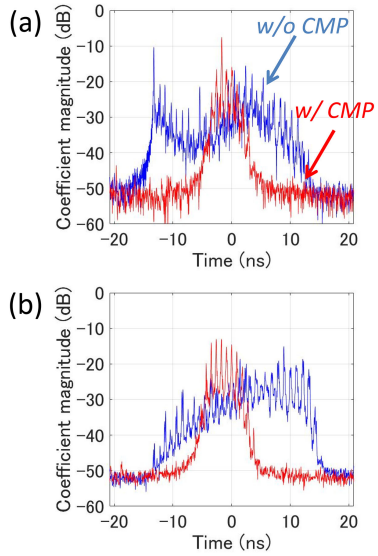

Fig. 7. Pulse broadening in the cases with (red) and without (blue) CMP scheme after transmission over 510 km for (a) LP_{01} mode and (b) LP_{11} mode.

difference smaller than 1 cm (corresponding to ∼50 ps/loop). The averaged optical power launched into the FMF was set to −2.5 dBm/mode/channel. At the end of each recirculating loop, the output ports were mutually switched with each other to apply a CMP transmission scheme where spatial channels are transmitted by a different spatial mode in each span in a cyclic manner. The transmitted signals were labeled mode 1, 2, and 3 and were input respectively to the mode MUX ports of LP_{01} LP_{11a}, and LP_{11b} at the initial span.

After transmission, the signals were detected by a 3-array coherent receiver module, and 1.6 M samples were stored into a 12-ch digital storage oscilloscope (DSO). Four subcarriers were then processed in parallel, each containing front-end error correction, chromatic dispersion compensation, and 6×6 frequency-domain MIMO equalization. The parallel signal transmission technique combined with the CMP enabled the equalizer tap number to be reduced to 896 even after 3060-km transmission in a DMD unmanaged FMF transmission line. Although an employment of a larger number of subcarriers would offer MIMO-DSP with smaller equalizer taps, it might also cause degradation in laser linewidth tolerance and enhancement of peak-to-average power ratio (PAPR) of signal waveforms. After bit-wise log-likelihood ratios were obtained through a soft demapper, LDPC decoding was performed by employing a log-domain sum product algorithm with ten iterations. Finally, the Q-factors were calculated by using 0.52 Mbits per spatial channel for both before and after LDPC decoding.

IV. Experimental Results

A. Pulse Broadening Suppression by CMP Scheme

Figs. 5(a) and (b) show respectively the optical spectrum measured before and after transmission over 3060 km. We confirmed that the signal power difference was within the range of ±3 dB even after 3060-km FMF transmission because of the employment of GFFs. Fig. 6 shows relative inverse group velocity between LP_{01} and LP_{11} in the FMF used in this experiment, which clarifies that DMD varies in the range from 33.7 to 44.3 ps/km across the C-band. The figure also indicates that the phase-matching condition between nondegenerate modes for the inter-modal four-wave mixing process may be satisfied over almost the entire transmission wavelength with a channel separation of 2 nm [29]. Then we evaluated a pulse suppression effect by using the CMP scheme at the center wavelength channel #44. The result is represented in Fig. 7. Note that small distinct peaky highs that appeared in the impulse responses were originated at the splice points between FMF devices, and that impulse responses are averaged within mode groups; for example, the impulse response for LP_{01} mode is obtained by taking an average over those of LP_{01X} and LP_{01Y}. In the transmission case where the CMP scheme was not employed, pulse energy peaks were respectively located at around −13.5 ns for LP_{01} mode and at around 9 ns for LP_{11} mode, yielding pulse spread larger than 20 ns even after 510 km transmission. When we switched to transmission with the CMP scheme, pulse energy was well concentrated in the window range as small as 10 ns. Fig. 8 compares the pulse broadening between the cases with and without the CMP scheme at three different channels (#1, #44,

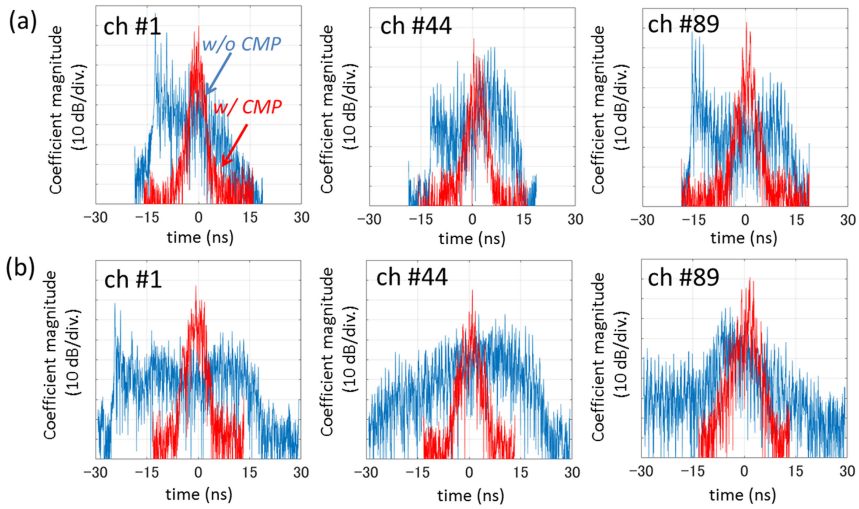

Fig. 8. Pulse broadening in the cases with (red) and without (blue) CMP scheme after transmission over 510 km (a) and 1020 km (b) at channels #1 (1529.56 nm), #44 (1546.52 nm), and #89 (1564.68 nm).

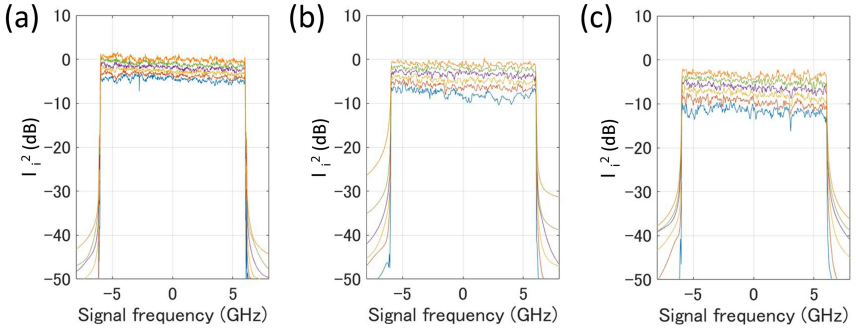

Fig. 9. Evolution of singular value distribution along FMF links at the center wavelength channel #44 at the distances of (a) 1020 km, (b) 2040 km, and (c) 3060 km.

and #89). In conventional transmission without using the CMP scheme, the memory length required for MIMO equalization in channel #89 expanded over 40 ns after 1020-km transmission because of DMD-unmanaged FMF links, while with CMP it was kept smaller than 15 ns over the entire C-band. These results lead us to conclude that applying of the CMP scheme to wideband FMF transmission is quite beneficial in mitigating DMD-induced pulse broadening even without an employment of DMD-management approach.

B. MDL and OSNR Characteristics

Next we investigated MDL and OSNR characteristics. We first estimated the channel transfer matrix after 3060 km transmission on the basis of the least squares method. Fig. 9 shows the obtained evolutions of singular values λ_i for six spatial channels in a signal bandwidth at the center wavelength channel (#44) that was calculated based on singular value decomposition of the channel transfer matrix. Note that the singular value slopes against frequency were originated from the electrical bandwidth limitation at the transmitter. Then the MDL in dB unit was estimated as MDL $= 10\log_{10}\lambda_{\max}^2/\lambda_{\min}^2$, where $\lambda_{\max}$ and $\lambda_{\min}$ are maximum and minimum singular values, respectively. The obtained overall MDL characteristics at each transmission reach are summarized in Fig. 10, which were obtained by taking average over signal bandwidth with respect to MDL values at each frequency. MDL value of 1.74 dB was observed after the initial span transmission that contained a pair of mode MUX/DEMUX devices and some FM splicing points. The growth of overall MDL and the standard deviation of MDL (σ_{MDL}) represented

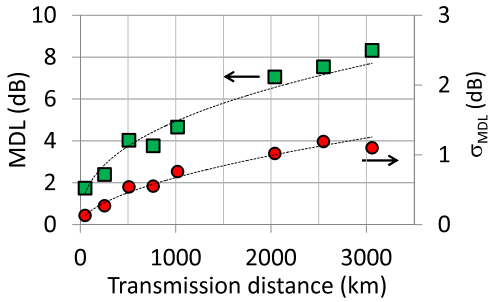

Fig. 10. Estimated overall MDL values and the standard deviations of MDL (σ_{MDL}) as a function of transmission distance at the center wavelength channel #44.

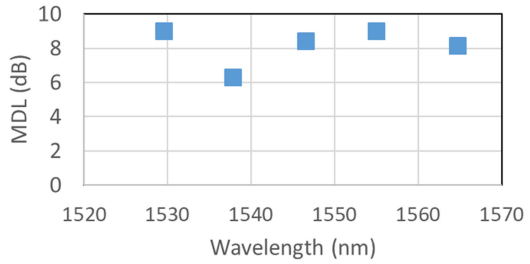

Fig. 11. Estimated MDL values after 3060-km transmission at channels #1, #22, #44, #65, and #89.

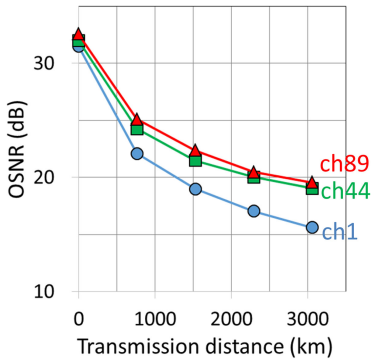

Fig. 12. Measured OSNR values at channels #1, #44, and #89.

a nonlinear property, which was agreed with theoretical studies for strongly-coupled MDM transmission regimes [30]. MDL values after 3060-km transmission at five different wavelength channels are shown in Fig. 11. The results shown in Figs. 10 and 11 indicated that the MDL value was suppressed to well below 10 dB over the C band even after 3060-km transmission, although the largest MDL was observed at channel #1. Although not shown in the presented paper, we also performed MDL performance comparison between cases with and without the CMP scheme. The results indicated that the CMP scheme does not seem affect overall MDL of the transmission link significantly. One possible reason for this is that the major origins of MDL in our setup were loop components rather than FMF and mode devices; since power optimization for loop systems was independently performed in each transmission case, MDL performance comparison might not be properly performed. We have previously clarified that MDL-impact mitigation was obtained by employing the CMP scheme in a sense that signal performance difference between spatial channels were clearly suppressed by the introduction of the scheme (see Fig. 9 in [14]). The further research would be needed on this issue. The measured OSNR values (0.1-nm resolution) at these channels are shown in Fig. 12, indicating that OSNR was also deteriorated at channel #1.

C. Signal Performance

Signal performance with various transmission distances at channels #1, #44, and #89 is compared in Fig. 13. The figure shows that in channel #1 the signal performance was more severely degraded than in the other channels, whose result agreed

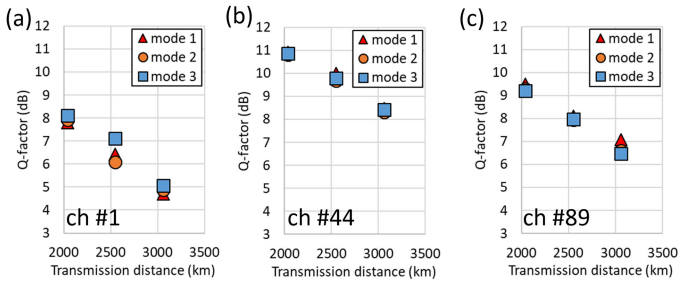

Fig. 13. Measured Q-factors as a function of transmission distance at channels (a) #1, (b) #44, and (c) #89.

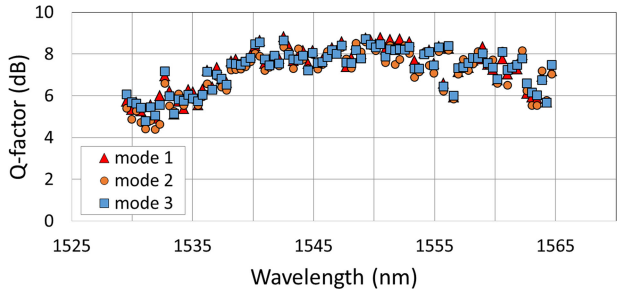

Fig. 14. Measured pre-LDPC Q-factors after 3060-km FMF transmission for all wavelength and spatial channels.

TABLE II
CHANNEL COUNTS FOR EACH FEC CODE RATE

FEC with LDPC code rate R	Net bit rate (Gb/s)	Number of spatial channels
CI-BCH + LDPC (R= 2/3)	119.12	39
CI-BCH + LDPC (R= 3/4)	134.01	3
CI-BCH + LDPC (R= 4/5)	142.94	89
CI-BCH + LDPC (R= 5/6)	148.90	6
CI-BCH + LDPC (R= 9/10)	160.81	96
CI-BCH only	178.68	34

with our evaluation of MDL and OSNR characteristics. We infer that the origin of degradation in the shorter wavelength channels was the increased noise figure and MDL in those channels due to the characteristics of employed discrete EDFAs and GFFs. We also found from Fig. 13 that the Q-factor difference between spatial channels was well suppressed within the range of $\pm$ 0.5 dB by using the CMP transmission scheme. Fig. 14 summarizes the obtained Q-factors for all 89 $\times$ 3 wavelength/spatial channels before LDPC decoding after 3060-km FMF transmission We also confirmed that all the post-LDPC Q-factors of these channels exceeded the FEC limit of 8.3 dB for the CI-BCH code [28]. Channel counts of each LDPC code rate are represented in Table II, from which we calculated the achieved net capacity was 40.18 Tb/s.

V. CONCLUSION

In this paper, we reported how we successfully demonstrated full C-band 40.18-Tb/s fewmode fiber (FMF) transmission over 3060 km, the longest distance yet reported without employing

differential mode delay (DMD)-management approach. Transmission with a cyclic mode permutation (CMP) scheme, which induces deliberate mode conversion in each span, was shown to mitigate the DMD impact in wideband FMF transmission across the 4.4-THz optical bandwidth. This enabled long-distance high-capacity transmission in a DMD-unmanaged FMF transmission link. We believe that the presented feature will prove to be advantageous in long-haul terrestrial FMF transport systems.

REFERENCES

[1] T. Morioka, "New generation optical infrastructure technologies: EXAT initiative towards 2020 and beyond," in *Proc. 14th OptoElectronics Commun. Conf.*, Jul. 2009, pp. 13–17.

[2] T. Kobayashi *et al.*, "1-Pb/s (32 SDM/46 WDM/768 Gb/s) C-band dense SDM transmission over 205.6-km of single-mode heterogeneous multi-core fiber using 96-Gbaud PDM-16QAM channels," in *Proc. 40th Opt. Fiber Commun. Conf. Exhib.*, Los Angeles, CA, USA, Mar. 2017, Paper Th5B.1.

[3] B. J. Puttnam *et al.*, "2.15 Pb/s transmission using a 22 core homogeneous single-mode multi-core fiber and wideband optical comb," in *Proc. 41st Eur. Conf. Opt. Commun.*, Valencia, Spain, Sep. 2015, Paper PDP.3.1.

[4] D. Soma *et al.*, "10.16 peta-bit/s dense SDM/WDM transmission over low-DMD 6-mode 19-core fibre across C + L band," in *Proc. 43rd Eur. Conf. Opt. Commun.*, Gothenburg, Sweden, Sep. 2017, Paper Th.PDP.A.1.

[5] R. Ryf *et al.*, "High-spectral-efficiency mode-multiplexed transmission over graded-index multimode fiber," in *Proc. 44th Eur. Conf. Exhib. Opt. Commun.*, Roma, Italy, Sep. 2018, Paper Th3B.1.

[6] T. Sakamoto *et al.*, "120 spatial channel few-mode multi-core fibre with relative core multiplicity factor exceeding 100," in *Proc. 44th Eur. Conf. Exhib. Opt. Commun.*, Roma, Italy, Sep. 2018, Paper We3E.5.

[7] G. Rademacher *et al.*, "159 Tbit/s C+L band transmission over 1045 km 3-mode graded-index few-mode fiber," in *Proc. 43rd Opt. Fiber Commun. Conf. Exhib.*, San Diego, CA, USA, Mar. 2018, Paper Th4C.4.

[8] J. van Weerdenburg *et al.*, "138-Tb/s mode- and wavelength-multiplexed transmission over six-mode graded-index fiber," *J. Lightw. Technol.*, vol. 36, no. 6, pp. 1369–1374, Mar. 2018.

[9] G. Rademacher *et al.*, "3500-km mode-multiplexed transmission through a three-mode graded-index few-mode fiber link," in *Proc. 43rd Eur. Conf. Opt. Commun.*, Gothenburg, Sweden, Sep. 2017, Paper M.2.E.4.

[10] Y. Sasaki, K. Takenaga, S. Matsuo, K. Aikawa, and K. Saitoh, "Few-mode multicore fibers for long-haul transmission line," *Opt. Fiber Technol.*, vol. 35, pp. 19–27, 2017.

[11] R. Ryf *et al.*, "Long-distance transmission over coupled-core multicore fiber," in *Proc. 42nd Eur. Conf. Opt. Commun.*, Dusseldorf, Germany, Sep. 2016, Paper Th.3.C.3.

[12] J. Fang, A. Li, and W. Shieh, "Low-DMD few-mode fiber with distributed long-period grating," *Opt. Lett.*, vol. 40, no. 17, pp. 3937–3940, Sep. 2015.

[13] H. Liu, H. Wen, R. Amezcua-Correa, P. Sillard, and G. Li, "Reducing group delay spread in a 9-LP mode FMF using uniform long-period gratings," in *Proc. 40th Opt. Fiber Commun. Conf. Exhib.*, Los Angeles, CA, USA, Mar. 2017, Paper Tu2J.5.

[14] K. Shibahara *et al.*, "DMD-unmanaged long-haul SDM transmission over 2500-km 12-core × 3-mode MC-FMF and 6300-km 3-mode FMF employing intermodal interference cancelling technique," in *Proc. 43rd Opt. Fiber Commun. Conf. Exhib.*, San Diego, CA, USA, Mar. 2018, Paper Th4C.6.

[15] K. Shibahara *et al.*, "Full C-band 3060-km DMD-unmanaged 3-mode transmission with 40.2-Tb/s capacity using cyclic mode permutation," in *Proc. 44th Opt. Fiber Commun. Conf. Exhib.*, San Diego, CA, USA, Mar. 2019, Paper W3F.2.

[16] E. Ip *et al.*, "146λ × 6 × 19-Gbaud wavelength-and mode-division multiplexed transmission over 10 × 50-km spans of few-mode fiber with a gain-equalized few-mode EDFA," *J. Lightw. Technol.*, vol. 32, no. 4, pp. 790–797, Nov. 2014.

[17] K. Shibahara *et al.*, "Iterative unreplicated parallel interference canceler for MDL-tolerant dense SDM (12-core × 3-mode) transmission over 3000 km," in *Proc. 44th Eur. Conf. Exhib. Opt. Commun.*, Roma, Italy, Sep. 2018, Paper Tu3F.6.

[18] R. Ryf *et al.*, "Photonic-lantern-based mode multiplexers for few-mode-fiber transmission," in *Proc. 39th Opt. Fiber Commun. Conf. Exhib.*, San Francisco, CA, USA, Mar. 2014, Paper W4J.2.

[19] R. Ryf *et al.*, "Distributed Raman amplification based transmission over 1050-km few-mode fiber," in *Proc. 41st Eur. Conf. Opt. Commun.*, Valencia, Spain, Sep. 2015, Paper Tu.3.2.3.

[20] R. Ryf *et al.*, "708-km combined WDM/SDM transmission over few-mode fiber supporting 12 spatial and polarization modes," in *Proc. 39th Eur. Conf. Exhib. Opt. Commun.*, London, U.K., Sep. 2013, Paper We.2.D.1.

[21] R. Ryf *et al.*, "10-mode mode-multiplexed transmission over 125-km single-span multimode fiber," in *Proc. 41st Eur. Conf. Opt. Commun.*, Valencia, Spain, Sep. 2015, Paper PDP 3.3.

[22] N. K. Fontaine *et al.*, "30 × 30 MIMO transmission over 15 spatial modes," in *Proc. 40th Opt. Fiber Commun. Conf. Exhib.*, Los Angeles, CA, USA, Mar. 2015, Paper Th5C.1.

[23] R. Ryf *et al.*, "Mode-multiplexed transmission over 36 spatial modes of a graded-index multimode fiber," in *Proc. 44th Eur. Conf. Exhib. Opt. Commun.*, Roma, Italy, Sep. 2018, Paper Tu1G.2.

[24] Mizuno *et al.*, "12-core × 3-mode dense space division multiplexed transmission over 40 km employing multi-carrier signals with parallel MIMO equalization," in *Proc. 39th Opt. Fiber Commun. Conf. Exhib.*, San Francisco, CA, USA, Mar. 2014, Paper Th5B.2.

[25] K. Shibahara *et al.*, "Dense SDM (12-core × 3-mode) transmission over 527 km with 33.2-ns mode-dispersion employing low-complexity parallel MIMO frequency-domain equalization," *J. Lightw. Technol.*, vol. 34, no. 1, pp. 196–204, Jan. 2016.

[26] J. Sakaguchi *et al.*, "Realizing a 36-core, 3-mode fiber with 108 spatial channels," in *Proc. 40th Opt. Fiber Commun. Conf. Exhib.*, Los Angeles, CA, USA, Mar. 2015, Paper Th5C.2.

[27] K. Igarashi *et al.*, "114 space-division-multiplexed transmission over 9.8-km weakly-coupled-6-mode uncoupled-19-core fibers," in *Proc. 40th Opt. Fiber Commun. Conf. Exhib.*, Los Angels, CA, USA, Mar. 2015, Paper Th5C.4.

[28] F. Chang, K. Onohara, and T. Mizuochi, "Forward error correction for 100 G transport networks," *IEEE Commun. Mag.*, vol. 48, no. 3, pp. S48–S55, Mar. 2010.

[29] R. Essiambre *et al.*, "Experimental investigation of inter-modal four-wave mixing in few-mode fibers," *IEEE Photon. Technol. Lett.*, vol. 25, no. 6, pp. 539–542, Mar. 2013.

[30] K.-P. Ho and J. M. Kahn, "Mode-dependent loss and gain: Statistics and effect on mode-division multiplexing," *Opt. Express*, vol. 19, pp. 16612–16635, Aug. 2011.

Kohki Shibahara (M'15) received the B.S. degree in physics, the M.S. degree in geophysics, and the Ph.D. degree in informatics from Kyoto University, Kyoto, Japan, in 2008, 2010, and 2017, respectively.

He joined NTT Network Innovation Laboratories, Yokosuka, Japan, in 2010. His current research interests include spatial division multiplexing transmission systems and advanced multiple-input and multiple-output signal processing. He is a Member of the IEICE and the IEEE/Photonics Society. He received the Tingye Li Innovation Prize from the OSA in 2016 and the Young Researcher's Award from the IEICE in 2017.

Takayuki Mizuno (M'04) received the B.E. degree in applied physics, the M.E. degree in crystalline materials science, and the Dr. Eng. degree in quantum engineering, all from Nagoya University, Nagoya, Japan, in 1998, 2000, and 2007, respectively.

In 2000, he joined NTT Photonics Laboratories, NTT Corporation, Japan, where he was involved in the research and development of silica planar lightwave circuit optical waveguide devices, including arrayed-waveguide gratings, Mach-Zehnder interferometer-based filters and switches, and digital coherent demodulators for advanced modulation formats. Since 2013, he has been a Senior Research Engineer with NTT Network Innovation Laboratories, NTT Corporation, Yokosuka. His current research interest includes space-division multiplexed transmission technology for ultrahigh-capacity optical transport systems.

Dr. Mizuno is a Member of the IEEE Photonics Society, the Optical Society (OSA), and the Institute of Electronics, Information, and Communication Engineers (IEICE). He is currently serving in the Technical Program Committee of the Optical Fiber Communication Conference.

Hiroto Kawakami (M'03) received the B.S. and M.S. degrees in physics from Kyoto Industrial University, Kyoto, Japan, and Hokkaido University, Sapporo, Japan, in 1989 and 1991, respectively.

In 1991, he joined the NTT Transmission Laboratories, Yokosuka, Japan, where he was involved in the research and development of high-speed optical communication systems. His research interest includes nonlinear effect in optical fiber and device control in transmission system. He is a Member of the Communication Engineers (IEICE) of Japan.

Takayuki Kobayashi (S'05–M'06) received the B.E. and M.E. degrees in communication engineering from Waseda University, Tokyo, Japan, in 2004, and 2006, respectively.

Since April 2006, he has been with the NTT Network Innovation Laboratories, NTT, Yokosuka, Japan. His current research interests include modulation formats, coherent detection, and high-speed fiber-optic communications systems. He is a Member of the Institute of Electronics, Information, and Communication Engineers (IEICE) of Japan and the IEEE/Photonics Society.

Masanori Nakamura received the B.S. and M.S. degrees in applied physics from Waseda University, Tokyo, Japan, in 2011 and 2013, respectively. In 2013, he joined NTT Network Innovation Laboratories, Yokosuka, Japan. He has been engaged in the research on high-capacity optical transport networks. His research interests include digital signal processing and modulation format optimization for high-speed optical transmission. He is a Member of the Institute of Electronics, Information, and Communication Engineers (IEICE) of Japan. He was the recipient of the 2016 IEICE Communications Society Optical Communication Systems Young Researcher's Award.

Kota Shikama (M'14) received the B.E. and M.E. degrees in materials science from Keio University, Kanagawa, Japan, in 2008 and 2010, respectively. He joined NTT Photonics Laboratories, Atsugi, Kanagawa, Japan, in 2010. He has been conducting research on optical packaging technologies for space division multiplexing components and high port-count wavelength selective switches. He received the Young Award from the IEEE Components, Packaging, and Manufacturing Technology Symposium, Japan in 2012. He received the Young Engineer Award from the Institute of Electronics, Information, and Communication Engineers (IEICE) of Japan in 2013. He is a Member of the IEICE.

Kazuhide Nakajima received the M.S. and Ph.D. degrees in electrical engineering from Nihon University, Chiba, Japan, in 1994 and 2005, respectively. In 1994, he joined NTT Access Network Systems Laboratories, Tokai, Ibaraki, Japan, where he is engaged in the research on optical fiber design and related measurement techniques. He is currently a Group Leader (Senior Distinguished Researcher) with the NTT Access Network Service Systems Laboratories, Tsukuba, Ibaraki. He is acting as a Rapporteur of Q5/SG15 of ITU-T since 2009. He is a Member of the Optical Society (OSA), the Institute of Electronics, Information, and Communication Engineers (IEICE) of Japan, and the Japan Society of Applied Physics (JSAP).

Yutaka Miyamoto (M'93) received the B.E. and M.E. degrees in electrical engineering from Waseda University, Tokyo, Japan, in 1986 and 1988, respectively, and the Dr.Eng. degree in electrical engineering from the University of Tokyo, Tokyo, Japan. In 1988, he joined NTT Transmission Systems Laboratories, where he was engaged in the R&D of high-speed optical communications systems including the first 10-Gbit/s terrestrial optical transmission system (FA-10 G) using EDFA (erbium-doped optical fiber amplifier) inline repeaters. He was with NTT Electronics Technology Corporation from 1995 to 1997, where he worked on the planning and product development of high-speed optical modules at data rates of 10 Gbit/s and beyond. Since 1997, he has been with the NTT Network Innovation Labs, where he has been researching and developing optical transport technologies based on 40/100/400-Gbit/s channels and beyond. He has also been investigating and promoting a scalable optical transport network with Pbit/s-class capacity based on innovative transport technologies such as digital signal processing, space division multiplexing, and cutting-edge integrated devices for photonic preprocessing. He currently serves as the Chair of the IEICE Technical Committee of Extremely Advanced Optical Transmission (EXAT). He is a Fellow of the IEICE.